Reductive Cleavage of Carbon Tetrachloride in a Polar Solvent. An Example of a Dissociative Electron Transfer with Significant Attractive Interaction between the Caged Product Fragments

Laurence Pause, Marc Robert, and Jean-Michel Savéant*

Contribution from the Laboratoire d'Electrochimie Moléculaire, Unité Mixte de Recherche Université−CNRS No. 7591, Université de Paris 7−Denis Diderot, 2 place Jussieu, 75251 Paris Cedex 05, France

Received April 10, 2000. Revised Manuscript Received July 6, 2000

Abstract: The electrochemical reduction of carbon tetrachloride in *N*,*N*′-dimethylformamide follows a mechanism in which electron transfer and bond cleavage are concerted, at least at low and moderate driving forces. A detailed analysis of the kinetics of the reductive cleavage reveals that a small but significant interaction between the Cl^- and $Cl_3C^•$ fragments exists in the product state and is responsible for a strong acceleration of the reaction. An extension of the theory of dissociative electron transfer is proposed to rationalize the kinetic results and estimate the magnitude of the interaction energy. The model explains how a relatively small interaction energy results in a substantial acceleration of the reaction, caused by both an increase of the driving force and a decrease of the intrinsic barrier. Due to the strong polarization of the CCl_3 radical, the reaction is a particularly clear example of the possibility that attractive interactions between fragments survive in a polar solvent. Another attractive feature of this example is that CCl_4 is small enough a molecule for the application of ab initio techniques, with electron correlation implementation, to be applicable, serving as a complement to the semiempirical model describing the effect of interactions between product fragments on the dynamics of dissociative electron-transfer reactions.

The mechanism and dynamics of reactions where single electron transfer triggers the breaking of a chemical bond is an important issue in the general understanding of chemical reactivity. They can be investigated in the framework of thermal heterogeneous (electrochemical) and homogeneous reactions[1] or of photoinduced processes.[2]

Two types of mechanisms have been identified: a stepwise mechanism in which electron transfer and bond breaking are successive, and a dissociative electron mechanism in which they are concerted. The dichotomy is as represented in Scheme 1, where the case of a reduction has been taken as an example. The existence of two different mechanisms is well documented for homogeneous and heterogeneous (electrochemical) thermal reactions.[1] A particularly clear distinction between these two reaction pathways can be made when the passage from one to the other can be experimentally characterized. Such changes of mechanism have been observed within families of cleaving substrates upon varying their molecular properties.[3] The main factors governing the mechanism dichotomy in this respect have been identified.[3] Even more striking is the prediction[4a] and observation that the mechanism changes from concerted to stepwise upon increasing the thermodynamic driving force offered to the reaction, as exemplified by an increasing number of cleaving substrates.[3c,4b−d]

Scheme 1

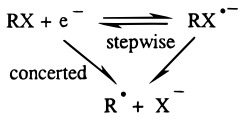

The electron step in the stepwise process is of the outer-sphere type. Its dynamics may therefore be rationalized using the Marcus−Hush model.[5] In the case of a concerted mechanism, the dissociative electron-transfer Morse curve model may be applied, as has already been done in several cases.[1a−c,6] In the original version of the model, the potential energy profile of

(1) (a) Savéant, J.-M. Single Electron Transfer and Nucleophilic Substitution. In *Advances in Physical Organic Chemistry*; Bethel, D., Ed.; Academic Press: New York, 1990; Vol. 26, pp 1−130. (b) Savéant, J.-M. Dissociative Electron Transfer. In *Advances in Electron Transfer Chemistry*; Mariano, P. S., Ed.; JAI Press: New York, 1994; Vol. 4, pp 53−116. (c) Savéant, J.-M. *Acc. Chem. Res.* **1993**, *26*, 455. (d) Lund, H.; Daasbjerg, K.; Lund, T.; Pedersen, S. U. *Acc. Chem. Res.* **1995**, *28*, 313. (e) Lund, H.; Daasbjerg, K.; Lund, T.; Occhialini, D.; Pedersen, S. U. *Acta Chem. Scand*. **1997**, *51*, 135.

(2) (a) Saeva, F. D. *Top. Curr. Chem.* **1990**, *156*, 61. (b) Saeva, F. D. Intramolecular Photochemical Electron Transfer (PET)−Induced Bond Cleavage Reactions in Some Sulfonium Salts Derivatives. In *Advances in Electron Transfer Chemistry*; Mariano, P. S., Ed.; JAI Press: New York, 1994; Vol. 4, pp 1−25. (c) Gaillard, E. R.; Whitten, D. G. *Acc. Chem. Res.* **1996**, *29*, 292.

(3) (a) Andrieux, C. P.; Le Gorande, A.; Savéant, J.-M. *J. Am. Chem. Soc.* **1992**, *114*, 6892. (b) Andrieux, C. P.; Differding, E.; Robert, M.; Savéant, J.-M. *J. Am. Chem. Soc.* **1993**, *115*, 6592. (c) Andrieux, C. P.; Robert, M.; Saeva, F. D.; Savéant, J.-M. *J. Am. Chem. Soc.* **1994**, *116*, 7864. (d) Andrieux, C. P.; Tallec, A; Tardivel, R.; Savéant, J.-M.; Tardy, C. *J. Am. Chem. Soc.* **1997**, *119*, 2420.

(4) (a) Andrieux, C. P.; Savéant, J.-M. *J. Electroanal. Chem*. **1986**, *205*, 43. (b) Antonello, S.; Maran, F. *J. Am. Chem. Soc*. **1997**, *119*, 12595. (c) Pause, L.; Robert, M.; Savéant, J.-M. *J. Am. Chem. Soc.* **1999**, *121*, 7158. (d) Antonello, S.; Maran, F. *J. Am. Chem. Soc*. **1999**, *121*, 9668.

(5) (a) Marcus, R. A. *J. Chem. Phys*. **1956**, *24*, 4966. (b) Hush, N. S. *J. Chem. Phys*. **1958**, *28*, 962. (c) Marcus, R. A. In *Special Topics in Electrochemistry*; Rock, P. A., Ed.; Elsevier: New York, 1977; pp 161−179.

(6) (a) Savéant, J.-M. *J. Am. Chem. Soc.* **1987**, *109*, 6788. (b) Savéant, J.-M. *J. Am. Chem. Soc.* **1992**, *114*, 10595. (c) Andrieux, C. P.; Savéant, J.-M.; Tardy, C.; Savéant, J.-M. *J. Am. Chem. Soc.* **1998**, *120*, 4167.

10.1021/ja001258s CCC: $19.00
Published on Web 09/22/2000

the product system is assumed to be purely repulsive, the interaction between the two fragments being regarded as negligible, at least in polar solvents.

There is indirect experimental evidence that such attractive interactions, of the charge/dipole type, may exist in the gas phase after injection of an electron in alkyl halides.[7] Ab initio calculations give contrasting results depending on the method used and approximations made.[8] It is usually assumed that these interactions vanish in polar solvents. One such case is the anionic state of CF_3Cl,[8b] where the shallow minimum calculated in the gas phase disappears upon solvation, at least when a simple continuum solvation model is used. The questions that arise are whether the attractive interaction existing in the gas phase may persist, even weakened, in the caged product system within a polar solvent, how its magnitude depends on the structure of $R^{\bullet}$ and X^-, and what its effect is on the dynamics of dissociative electron transfer.

Indications that such attractive interactions may, indeed, remain significant in polar solvents stem from observations made in the electron-transfer chemistry of substituted benzyl halides. Whereas the electrochemical reduction of 4-nitrobenzyl bromide in DMF is clearly a stepwise reaction, a concerted mechanism is observed with unsubstituted benzyl and 4-cyanobenzyl bromides.[3a] The cyclic voltammetric peak potential of 4-cyanobenzyl bromide is significantly more positive than the cyclic voltammetric peak potential of benzyl bromide (by 250 mV at a scan rate of 0.1 V/s). It was inferred from these observations that the bond dissociation energy increases by 0.15 eV from the first to the second compound, in line with previous photoacoustic work,[9a] in which the substituent effect was regarded as concerning the starting molecule rather than the radical. However, further measurements using the same technique did not detect any substituent effect, and the same conclusion was also reached in the gas phase by using a low-pressure pyrolysis technique.[9b] Recent quantum chemical estimations[9c] concluded that there is a small substituent effect, namely, 0.07 eV, i.e., about half of the value derived from electrochemical experiments upon application of the classical dissociative electron-transfer theory. These observations may be interpreted as due to a small attractive interaction between the caged product fragments that would be larger in the presence than in the absence of the cyano substituent because of its electron-withdrawing character. An even larger similar effect is observed with phenacyl chloride and bromide, as expected from the electron-withdrawing effect of the carbonyl group. The apparent bond dissociation energies derived from cyclic voltammetry[2d] are again significantly lower than the values derived from low-pressure pyrolysis.[9d]

Another interesting example of the existence of such attractive interactions between caged product fragments results from recent investigations of the initiation step in the Kornblum[10a] $S_{RN}1$ reactions of 2-nitropropanate ion with 4-nitrocumyl chloride and 4-nitrobenzyl chloride in acetonitrile.[10b,c] The fragments interact significantly in the case of 4-nitrobenzyl chloride, with an energy of ca. 0.1 eV, whereas they do not interact to any significant extent in the case of 4-nitrocumyl chloride, in line with steric and electronic effects.

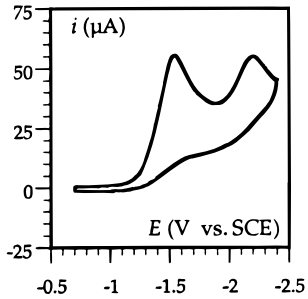

Figure 1. Cyclic voltammetry of CCl_4 (1.55 mM) in DMF + *n*-Bu_4NBF_4 at 294 K on a glassy carbon electrode. Scan rate: 0.2 V/s.

It is remarkable that a significant interaction between caged fragments seems to appear only with molecules where strong electron-withdrawing effects are present, thus reinforcing the charge/dipole (and induced dipole) between the anion leaving group and the radical, making it strong enough to compete with the shielding effect of the polar solvent. In this respect, the reductive cleavage of carbon tetrachloride seems an ideal case for investigating the problem since the electron-withdrawing effect of the three chlorine atoms in CCl_3 should result in a substantial interaction with Cl^- in the solvent cage.

Previous work on thermal electron transfer to CCl_4 in solution has led to contradictory conclusions as to the concerted or stepwise character of the reaction.[11] A first task of the work described below was thus to establish this point.

We will see that quantum chemical calculations prove useful for fully analyzing the dynamics of the dissociative electron transfer. CCl_4 is an attractive molecule in this respect, too, since it is small enough for the application of ab initio techniques with electron correlation implementation to remain tractable.

Results and Discussion

Figure 1 shows a typical cyclic voltammogram for the reduction of CCl_4 in *N*,*N*′-dimethylformamide (DMF). The first irreversible wave (which remains irreversible over the whole explored range of scan rates, i.e., up to 100 V/s) is a two-electron wave. The second, irreversible wave corresponds to the reduction of chloroform formed at the first wave, as checked with an authentic sample.[12] We may infer from these data that the reduction at the first wave follows the mechanism depicted in Scheme 2.[12] The second electron transfer is expected to take

(7) (a) Wentworth, W. E.; Becker, R. S.; Tung, R. *J. Phys. Chem.* **1967**, *71*, 752. (b) Wentworth, W. E.; George, R.; Keith, H. *J. Chem. Phys.* **1969**, *51*, 1791. (c) Steelhammer, J. C.; Wentworth, W. E. *J. Chem. Phys.* **1969**, *51*, 1802. (d) Chen, E. C. M.; Albyn, K.; Dussack, L.; Wentworth, W. E. *J. Phys. Chem.* **1989**, *93*, 6827. (e) Marcus, R. A. *Acta Chem. Scand*. **1998**, *52*, 858.

(8) (a) Benassi, R.; Bernardi, F.; Bottoni, A.; Robb, M. A.; Taddei, F. *Chem. Phys. Lett*. **1989**, *161*, 79. (b) Bertran, J.; Gallardo, I.; Moreno, M.; Savéant, J.-M. *J. Am. Chem. Soc*. **1992**, *114*, 9576. (c) Tada, T.; Yoshimura, R. J. *Am. Chem. Soc*. **1992**, *114*, 1593.

(9) (a) Clark, K. B.; Wayner, D. D. M. *J. Am. Chem. Soc*. **1991**, *113*, 9363. (b) Laarhoven, L. J. J.; Born, J. G. P.; Arends, I. W.; Mulder, P. *J. Chem. Soc., Perkin Trans. 2* **1997**, 2307. (c) Pratt, D. A.; Wright, J. S.; Ingold, K. U. *J. Am. Chem. Soc.* **1999**, *121*, 4877. (d) Dorrestijn, E.; Hemmink, S.; Hultsmaan, G.; Monnier, L.; Van Scheppingen, W.; Mulder, P. *Eur. J. Org. Chem.* **1999**, *607*, 7.

(10) (a) Kornblum, N. Angew. *Chem., Int. Ed. Engl.* **1975**, *14*, 734. (b) Costentin, C.; Hapiot, P.; Médebielle, M.; Savéant, J.-M. *J. Am. Chem. Soc.* **1999**, *121*, 4451. (c) Costentin, C.; Hapiot, P.; Médebielle, M.; Savéant, J.-M. *J. Am. Chem. Soc.* **2000**, *122*, 5623.

(11) (a) Eberson, L. *Acta Chem. Scand. B* **1982**, *36*, 533. (b) Eberson, L.; Ekstrom, M. *Acta Chem. Scand. B* **1988**, *42*, 113.

(12) (a) In agreement with a previously reported low-scan-rate voltammogram in the same medium at the same electrode.[12b] (b) Franz, R. N., III; Hasslinger, B. L.; Lambert, F. L. *J. Electrochem. Soc.* **1975**, *122*, 737. (c) Two other, more negative waves can be seen on the low-scan-rate voltammogram, corresponding to further reduction of chloroform in line with earlier polarographic and preparative-scale results.[12b] (d) In carefully dried solvent, the formation of dichlorocarbene by expulsion of Cl^- from Cl_3Cl^- competes with its protonation.[12e,f] (e) Duty, J.; Wawzonek, S. *J. Electrochem. Soc.* **1961**, *108*, 1135. (f) Fritz, H. P.; Kornrumpf, W. *Liebigs Ann. Chem.* **1978**, 1476.

Scheme 2

$$CCl_4 + e^- \longrightarrow Cl_3C^{\bullet} + Cl^-$$
$$Cl_3C^{\bullet} + e^- \rightleftharpoons Cl_3C^-$$
$$Cl_3C^- + H^+ \longrightarrow Cl_3CH$$

place at a potential much more positive than the first,[13] which thus appears as the rate-determining step of the whole reaction. The peak width and peak potential characteristics thus reflect solely the kinetics of the first electron-transfer step with no interference of the second electron transfer. The peak width, $E_{p/2} - E_p$ (E_p, peak potential; $E_{p/2}$, half-peak potential) of the first wave is large (of the order of 120 mV), as expected for a slow charge transfer. The transfer coefficient (symmetry factor) may be obtained from either the peak width or the variation of the peak potential with the scan rate (υ) according to the following equation.[14]

$$\alpha = (1.86RT/F)/(E_{p/2} - E_p)$$
$$= -(RT/2F)/(\partial E_p/\partial \ln \upsilon)$$

From peak width measurements, α is thus found to be equal to 0.34 between 0.05 and 1 V/s, falling in line within experimental uncertainty with the value 0.35−0.36 derived from peak potential variations with scan rate between 0.05 and 10 V/s. At 0.1 V/s, the peak is located at −1.56 V vs SCE. The peak location and the transfer coefficient are the two observables that serve to test the models of the electrochemical reductive cleavage that is to be discussed now.

Linearization of the electron-transfer kinetic law over the potential covered by the cyclic voltammetric wave at a fixed scan rate leads to the following expression for the free energy of activation at the peak.[1a,b]

$$\Delta G^{\ddagger} = \frac{RT}{F}\left[\ln\left(Z^{el}\sqrt{\frac{RT}{\alpha F \upsilon D}}\right) - 0.78\right]$$

$Z^{el} = \sqrt{RT/2\pi M} = 5 \times 10^3$ cm s^{-1} (M is molar mass) is the electrochemical collision frequency, υ is the scan rate, and D (10^{-5} cm^2 s^{-1}) the diffusion coefficient. The free energy of activation at the peak is thus found to be 0.338 eV.

We may examine first whether these data are consistent with a concerted mechanism in the framework of the dissociative electron transfer theory in its original version, where possible interactions between fragments in the product state are neglected.[1a−c,6] $\Delta G^{\ddagger}$ is obtained by free energy minimization on the intersection of the two surfaces,

$$G_{CCl_4 + e^-} = D_R Y^2 + \lambda_0(Y) X^2$$

$$G_{Cl_3C^{\bullet},Cl^-} = E_p - E^0 + D_R(1 - Y)^2 + \lambda_0(Y)\,(1 - X)^2$$

with $Y = 1 - \exp[-\beta(y - y_R)]$. X is a fictitious charge borne by the molecule, with a value between 0 and 1, serving as an index for solvent reorganization. $\beta = \nu(2\pi^2\mu/D)^{1/2}$ (y, bond length; y_R, equilibrium value of y in RX; ν, frequency of the cleaving bond; μ, reduced mass). E_p is the cyclic voltammetric potential. E^0, the standard potential for the dissociative electron-transfer reaction, can be obtained from the thermodynamic parameters present in the following equation.

$$E^0 = -D_R + E^0_{Cl^{\bullet}/Cl^-} + T(S_{CCl_3^{\bullet}} + S_{Cl^{\bullet}} - S_{CCl_4})$$

Estimation of the bond dissociation energy (2.84 eV),[15] of the entropic term (0.381 eV),[15e] and of the standard potential of the $Cl^{\bullet}/Cl^-$ couple in DMF (1.81 V vs SCE)[16] leads to $E^0 = -0.649$ V vs SCE. D_R is the dissociation energy of the cleaving bond. λ_0, the Marcus−Hush[5] solvent reorganization energy, is here a function of the progress of bond cleavage. It can be approximated by the following expression.[6c]

$$\lambda_0(Y) = (1 - Y)\lambda_0^R + Y\lambda_0^P$$

where λ_0^R and λ_0^P, the reorganization energies for the reactant and product states, may be obtained from $\lambda_0^{R,P}$ (eV) $= 3/a_{R,P}$ (Å), where $a_R = 3.17$ and $a_P = 1.81$ Å are the radii of CCl_4 and Cl^-, respectively. The activation free energy, $\Delta G^{\ddagger}$, is thus obtained by iteratively repeating the minimization procedure depicted above.[6c] The transfer coefficient, $\alpha = \partial\Delta G^{\ddagger}/\partial\Delta(E_p - E^0)$, is obtained by repeating the calculation for slightly different values of the driving force, i.e., of $E_p - E^0$. The values of both $\Delta G^{\ddagger}$ and α are too large as compared to the experimental values (see Table 1).

We are thus led to investigate the *possibility of an attractive interaction between the $Cl_3C^{\bullet}$ radical and the Cl^- in the product state and its effect on the reaction dynamics*. Such an attractive interaction does exist in the gas phase, as depicted in Figure 2.

(13) (a) The reduction potential of $Cl_3C^{\bullet}$ is not known. We estimated it from a comparison with the reduction potential of *t*-Bu$^{\bullet}$ [13b] according to the following procedure. The standard free enthalpy of the reaction $Cl_3C^{\bullet}$ + *t*-Bu$^-$ → Cl_3C^- + *t*-Bu$^{\bullet}$ was found to be equal to −2.4 eV by means of a quantum chemical ab initio calculation involving geometry optimization and energy calculation at the UHF-MP2 level, followed by a calculation of the standard free enthalpy of solvation according to the IPCM method, which defines a cavity for the solute as an electronic isodensity surface. The reduction potential of *t*-Bu$^{\bullet}$ is −2.2 V vs SCE.[13b] Assuming that the intrinsic barriers are not very different for the two reactions, we may conclude that the reduction potential of $Cl_3C^{\bullet}$ is ca. 0.2 V vs SCE, i.e., much more positive than the potential at which the reduction of CCl_4 occurs. (b) Andrieux, C. P.; Gallardo, I.; Savéant, J.-M. *J. Am. Chem. Soc.* **1989**, *111*, 1620.

(14) (a) Nadjo, L.; Savéant, J.-M. *J. Electroanal. Chem.* **1973**, *48*, 113. (b) Andrieux, C. P.; Savéant, J.-M. In *Electrochemical Reactions in Investigation of Rates and Mechanisms of Reactions, Techniques of Chemistry*; Bernasconi, C. F., Ed.; Wiley: New York, 1986; Vol. VI/4E, Part 2, pp 305−390.

(15) (a) Ab initio quantum chemical calculation of D_R (UHF-MP2, see the Methodology section) gave a value of 2.84 eV, in fair agreement with the experimental values of 2.86,[15b] 2.99,[15c] and 3.08.[15d] (b) *Handbook of Chemistry and Physics*, 78th Ed.; CRC: Cleveland, OH, 1997−1998. (c) Hudgens, J. W.; Johnson, R. D., III; Timonen, R. S.; Seetula, J. A.; Gutman, D. *J. Phys. Chem.* **1991**, *95*, 4400. (d) Chase, M. W., Jr. *Journal of Physical and Chemical Reference Data*; The American Chemical Society and The American Institute of Physics, 1998; Monograph 9, 4th Ed., Part 1. (e) From ab initio quantum chemical calculations (UHF-MP2, see the Methodology section), $T(S_{CCl_3^{\bullet}} + S_{Cl^{\bullet}} - S_{CCl_4}) = 0.381$ eV at the temperature of the experiments, 21 °C, taking into account that the standard states refer to 1 mol/L.

(16) (a) Standard redox potential of the $Cl^{\bullet}/Cl^-$ couple in DMF versus aqueous SCE was derived from the following expression:

$$E^{0,DMF}_{Cl^{\bullet}/Cl^-}(\text{vs SCE}) = E^{0,DMF}_{Cl^{\bullet}/Cl^-}(\text{vs Ag/Ag}^+) + E^{0,DMF}_{Ag^+/Ag}(\text{vs SCE})$$
$$= \mu^{0,DMF}_{Cl^{\bullet}} - \mu^{0,DMF}_{Cl^-} - \mu^{0,DMF}_{Ag^+} + \mu^0_{Ag} + 0.44$$
$$\approx \mu^{0,H_2O}_{Cl^{\bullet}} - (\mu^{0,H_2O}_{Cl^-} + \Delta_{trn}G^0_{Cl^-,H_2O\rightarrow DMF}) - (\mu^{0,H_2O}_{Ag^+} + \Delta_{trn}G^0_{Ag^+,H_2O\rightarrow DMF}) + \mu^0_{Ag} + 0.44$$
$$= E^{0,H_2O}_{Cl^{\bullet}/Cl^-}(\text{vs SHE}) - E^{0,H_2O}_{Ag^+/Ag}(\text{vs SHE}) - (\Delta_{trn}G^0_{Cl^-,H_2O\rightarrow DMF} + \Delta_{trn}G^0_{Ag^+,H_2O\rightarrow DMF}) + 0.44$$

Standard redox potentials in water versus SHE and standard free enthalpies of transfer from water to DMF, $\Delta_{trn}G^0_{X,H_2O\rightarrow DMF}$, were calculated from refs 15 and 16b. (b) Marcus, Y. *Ion Properties*; Marcel Dekker: New York, 1997.

Table 1. Comparison between Models and Experiment

	$\Delta G^{\ddagger}$ (eV)[a,b]	α[a]
experimental	0.338	0.34−0.35
model with no interaction between fragments	0.610	0.42
first model with interaction between fragments	0.514	0.39
second model with a −0.062 eV interaction between fragments	0.338	0.35

[a] At the peak, at 0.1 V/s. [b] In electronvolts.

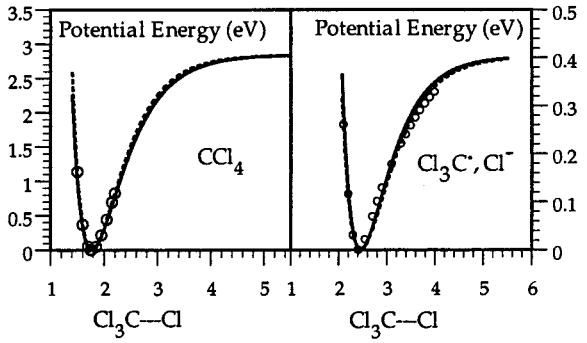

Figure 2. Potential energy profile of CCl_4 and $Cl_3C^{\bullet},Cl^-$ in the gas phase (distances in Å). ○: MP2 calculation. Solid lines: best-fit Morse curves with a common value of β (1.72 $Å^{-1}$) for CCl_4 and $Cl_3C^{\bullet},Cl^-$. Dotted lines: best-fit Morse curves with the best value of β for CCl_4 (1.81 $Å^{-1}$) and $Cl_3C^{\bullet},Cl^-$ (1.63 $Å^{-1}$) separately.

The geometries of the minimum on the potential energy curve and of the separated products, $Cl_3C^{\bullet} + Cl^-$, were optimized using several different methods. The geometries and energy parameters are summarized in Table 2. It is seen that in terms of both geometries and energies, the MP2 level of calculation provides a satisfactory approximation, as evidenced by the fact that upper levels of calculation such as MP3 and QCISD do not result in large variations. We therefore calculated the potential energy profile at the MP2 level for several different values of the length of the cleaving bond, optimizing the other coordinates under the constraint that the leaving chlorine atom remains on the axis of the pyramid formed by the three other chlorines. The variation of the electronic energy with the C- - -Cl distance shown in Figure 2 is thus obtained. It can be considered to a good approximation as the variation of the potential energy with the C- - -Cl distance. Indeed, as seen in Table 2, the variation of the electronic energy from the minimum to the separated fragments, 0.403 eV, is very close to the variation of the enthalpy, 0.409 eV. The points thus obtained may be fitted with the following Morse curve,

$$U_P = D_P\{1 - \exp[-\beta_P(y - y_P)]\}^2$$

with $D_P = 0.403$ eV, $y_P = 2.46$ Å, and $\beta_P = 1.63$ $Å^{-1}$. As can be seen on the left part of Figure 2, points obtained at the same calculation level for CCl_4 can also be fitted with a Morse curve,

$$U_R = D_R\{1 - \exp[-\beta_R(y - y_R)]\}^2$$

with $D_R = 2.84$ eV, $y_R = 1.77$ Å, and $\beta_R = 1.81$ $Å^{-1}$. It is worth noting that the shape factors, β, of the two Morse curves are very similar and that, as can be seen in Figure 2, the error made by fitting both curves with the same shape factor, $\beta = 1.72$ $Å^{-1}$, is negligible.[17] This observation confirms the validity of the approximation made in the theory of dissociative electron transfer that the repulsive term in the reactant and product systems are practically the same. To evaluate the effect of solvation on the potential energy vs bond length profiles and estimate the solvent reorganization energy, we may follow two different approaches.

In one of these, we used a dielectric continuum approximation (COSMO; see the Methodology for Quantum Chemical Calculations section). The solvation free energy of the negative state is also a function of the C- - -Cl distance. Figure 3b shows the variation of the solvation free energy of the negative state,

$$\Delta G^{solv}_{Cl_3C^{\bullet},Cl^-} = G^{solv}_{Cl_3C^{\bullet},Cl^-} - G^{solv}_{Cl_3C^{\bullet}+Cl^-}$$

with the C- - -Cl distance. The second term on the right-hand side corresponds to infinite separation of the fragments, i.e., essentially to the solvation of Cl^-. Addition of the solvation terms to the gas-phase electronic energy results in the disappearance of the energy minimum (Figure 3c). The resulting energy profile is, however, significantly different from a purely repulsive Morse profile (dotted line), except at short distances.

We may also derive the solvent reorganization free energy from the same calculation, using a value slightly smaller than the Hush approximation as previously discussed.[6c] Thus,

$$\lambda_0 = G^{solv}_{Cl_3C^{\bullet},Cl^-}\frac{3.00}{3.38}\frac{\frac{1}{\epsilon_{op}} - \frac{1}{\epsilon_S}}{1 - \frac{1}{\epsilon_S}} = 0.423G^{solv}_{Cl_3C^{\bullet},Cl^-} \qquad (1)$$

in the case of DMF.[16b] Here, ϵ_{op} and ϵ_S are the optical and static dielectric constants of the solvent, respectively. The variations of λ_0 with the C- - -Cl distance are shown in Figure 3d.

We may thus express the free energies of the reactant and product states by the following two equations.

$$G_{CCl_4 + e^-} = D_R\{1 - \exp[-\beta_R(y - y_R)]\}^2 + \lambda_0(y)X^2$$

$$G_{Cl_3C^{\bullet},Cl^-} = \Delta G^0 + D_P\{1 - \exp[-\beta_P(y - y_P)]\}^2 + \Delta G^{solv}_{Cl_3C^{\bullet},Cl^-}(y) + \lambda_0(y)(1 - X)^2$$

ΔG^0 is the standard free energy of the reaction from CCl_4 to the separated fragments, $Cl_3C^{\bullet} + Cl^-$ ($\Delta G^0 = E_p - E^{\circ}$ at the cyclic voltammetric peak). X is a fictitious charge serving as solvation index. The activation free energy, $\Delta G^{\ddagger}$, is obtained by minimization of the above two expressions subject to the condition $G_{CCl_4 + e^-} = G_{Cl_3C^{\bullet},Cl^-}$. From the difference between the two equations, one obtains

$$X^{\ddagger} = \frac{1}{2}\left[1 + \frac{\Delta G^0 + D_P\{1 - \exp[-\beta_P(y - y_P)]\}^2 - D_P}{\lambda_0(y)} - \frac{D_R\{1 - \exp[-\beta_R(y - y_R)]\}^2 + \Delta G^{solv}_{Cl_3C^{\bullet},Cl^-}(y)}{\lambda_0(y)}\right]$$

and from there, minimization of $\Delta G^{\ddagger}$,

$$\Delta G^{\ddagger} = D_R\{1 - \exp[-\beta_R(y - y_R)]\}^2 + \lambda_0(y)X^{\ddagger 2}$$

as a function of y leads to the value reported in Table 1. The predicted value of $\Delta G^{\ddagger}$ (which incidentally corresponds to $y^{\ddagger} = 2.04$ Å) is closer but still above the experimental value.

(17) (a) This is obviously not the case with empirical methods such as PM3,[17b] thus showing the weakness of these methods in the study of dissociative electron-transfer dynamics. (b) Tikhomirov, V. A.; German, E. D. *J. Electroanal. Chem.* **1998**, *450*, 13.

Table 2. Geometries and Energy Parameters

distances (Å) and angles (deg)	$Cl_3C^{\bullet},Cl^-$ minimum: PM3, UHF, MP2, MP3, QCISD	$Cl_3C^{\bullet} + Cl^-$ separated products PM3, UHF, MP2, MP3, QCISD	CCl_4 minimum: MP2, exptl [21d]
C- - -Cl	1.976, 3.127, 2.421, 2.477, 2.544		
C−Cl	1.763, 1.722, 1.780, 1.772, 1.770	1.640, 1.714, 1.713, 1.716, 1.719	1.77, 1.76
∠Cl−C−Cl	108.7, 115.6, 109.6, 110.5, 111.0	120.0, 117.1, 116.9, 117.1, 117.1	109.5, 109.5
charge on Cl	−0.53, −0.96, −0.71, −0.75, −0.79		
$Cl_3C^{\bullet},Cl^- \rightarrow Cl_3C^{\bullet} + Cl^-$			
electronic energies (ΔE in eV): PM3, UHF, MP2 (enthalpy), MP3, QCISD			
0.343, 0.176, 0.403 (0.409), 0.314, 0.338			

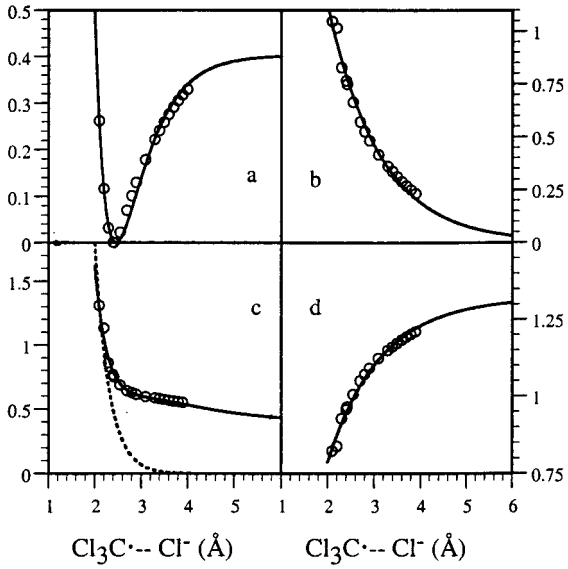

Figure 3. Interactions (in eV) between $Cl_3C^{\bullet},Cl^-$ and the solvent as a function of the $Cl_3C^{\bullet}-Cl^-$ distance (in Å). (a) Potential energy in the gas phase. The points are derived from ab initio UHF-MP2 calculations, and the solid line shows their fitting with a Morse curve (see text). (b) Solvation free energy in DMF according to the COSMO dielectric continuum model. (c) Sum of the energies in (a) and (b). Dotted line: repulsive part of the Morse curve. (d) Solvent reorganization energy, λ_0. In (a), (b), and (c), the origin on the energy axis corresponds to infinite separation of the fragments. The zero in (b) corresponds to a much lower energy than that in (a) (the difference is the solvation energy of the free Cl^- ion).

Taking into account the charge−induced dipole interaction between $Cl_3C^{\bullet}$ and Cl^- thus results in a significant but insufficient improvement of the modeling of the reaction dynamics. The lack of a stronger effect is related to the fact that, at the transition state, the product potential energy curve is very close to a purely repulsive Morse curve (Figure 3c). In fact, the decrease of the activation free energy as compared to that of the simple model is mostly due to a smaller value of λ_0 at the transition state, 0.80 instead of 0.94 eV.

The transfer coefficient, $\alpha = \partial\Delta G^{\ddagger}/\partial\Delta G^0$, was obtained from the same type of calculation by slightly varying ΔG^0 around is actual value. The value thus found (Table 1) is not far from the experimental values.

Dielectric continuum models of solvation such as the one used above are rather crude and not well suited to the description of short-range interactions between the ion and the discrete solvent molecules in the primary solvation shell. It follows that a shallow minimum in the potential energy vs C- - -Cl distance profile may well be missed by application of this type of solvation model. This is the reason that we will now describe an empirical model in which such a minimum exists and investigate how the activation free energy depends on its deepness. Our goal is simply to see whether small interactions of this sort are sufficient to significantly decrease the activation free energy and thus explain the observed kinetics.

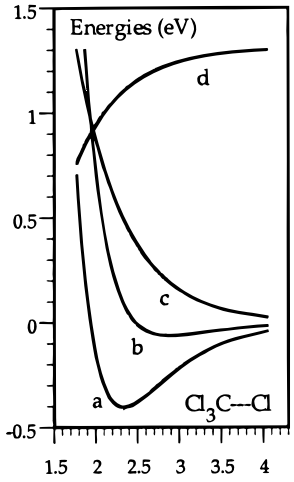

Figure 4. Energy profiles for $Cl_3C^{\bullet},Cl^-$ in DMF (distances in Å). (a) Potential energy in the gas phase. (b) Potential energy in the solvent ($D_P' = 62$ meV). (c) Variation of the solvation free energy. (d) Solvent reorganization energy. In (a) and (b), the origin on the energy axis corresponds to infinite separation of the fragments. The zero in (b) corresponds to a much lower energy than that in (a) (the difference is the solvation energy of the free Cl^- ion).

The reactant free energy may be represented, as before, by the following equation.

$$G_{CCl_4 + e^-} = D_R\{1 - \exp[-\beta_R(y - y_R)]\}^2 + \lambda_0(y)X^2$$

For the product profile we assume that in the solvent it has the shape of a Morse curve (Figure 4), as in the gas phase, albeit with a smaller value of the dissociation energy that we now note D_P' instead of D_P.

$$G_{Cl_3C^{\bullet},Cl^-} = \Delta G^0 - \Delta G^0_{sp} + D_P'\{1 - \exp[-\beta_P(y - y_P)]\}^2 + \lambda_0(y)(1 - X)^2$$

ΔG^0 is the standard free energy of the reaction leading to the separated fragments, and $\Delta G^0_{sp} = D_P' - T\Delta S^0_{sp}$ is the difference between the standard free energies of the separated and the caged fragments. We assume, as discussed earlier, that the two shape factors are the same, $\beta_R = \beta_P = \beta$, and that the repulsive terms in the two Morse curves are approximately the same. It follows that

$$y_P = y_R + \frac{1}{2\beta}\ln\left(\frac{D_R}{D_P'}\right)$$

indicating that a shallow minimum ($D_P' \ll D_R$) corresponds to

a loose cluster ($y_P \gg y_R$). Thus,

$$G_{CCl_4 + e^-} = D_R Y^2 + \lambda_0(Y)X^2 \quad (2)$$

$$G_{Cl_3C^\bullet,Cl^-} = \Delta G^0 - \Delta G^0_{sp} + D_R\left[\left(1 - \sqrt{\frac{D_P'}{D_R}}\right) - Y\right]^2 + \lambda_0(Y)(1 - X)^2 \quad (3)$$

with $Y = 1 - \exp[-\beta(y - y_R)]$.

The difference between the energy profiles in the solvent and in the gas phase provides us with the solvation free energy (profile c in Figure 4). We may also derive the solvent reorganization energy, λ_0, as a function of the C- - -Cl distance (profile d in Figure 4) by application of eq 1, taking $\Delta G^{solv}_{Cl_3C^\bullet + Cl^-} = 3.1$ eV.[16b] We thus know the function $\lambda_0(Y)$ in eqs 2 and 3. The value of X can be obtained as a function of Y for the transition state by combination of these two equations. The activation free energy is then obtained by the same minimization procedure as in the preceding model.

It appears that the effect of an attractive interaction between the fragments in the product cluster is not merely described by the introduction of a work term in the classical theory of dissociative electron transfer. Such a work term appears under the form of ΔG^0_{sp}, but there is also a modification of the intrinsic barrier. If the variation of λ_0 were neglected, the change in the intrinsic barrier would simply be obtained by replacement of D_R with $(\sqrt{D_R} - \sqrt{D_P'})^2$:

$$\Delta G^{\ddagger} \approx \frac{(\sqrt{D_R} - \sqrt{D_P'})^2 + \lambda_0}{4}\left[1 + \frac{\Delta G^0 - \Delta G^0_{sp}}{(\sqrt{D_R} - \sqrt{D_P'})^2 + \lambda_0}\right]^2$$

This effect is the most important factor in the decrease of the activation free energy.

The entropy of solvation in DMF is -175.7 J K^{-1} mol^{-1},[16b] corresponding to an entropy term of -0.535 eV at the temperature of the experiment. As seen before, the entropy term for the cleavage of the bond is 0.381 eV. From the energy minimum to the separated fragments, the entropy of solvation is expected to decrease, whereas the cleavage entropy increases. We may assume that these two variations approximately compensate each other and therefore that $\Delta G^0_{sp} \approx D_P'$.

Applying the above minimization procedure, we found that the experimental activation free energy can be reproduced by introduction of a rather small attractive interaction, namely, 62 meV. It is interesting to note that the transfer coefficient predicted in these conditions is in very good agreement with the experimental value (Table 1).

At this stage we may conclude that the electrochemical reductive cleavage to CCl_4 occurs, at low scan rates, according to a mechanism in which electron transfer and bond breaking are concerted. Analysis of the reaction dynamics revealed the existence of a charge−induced dipole interaction between the two fragments, $Cl_3C^\bullet$ and Cl^- in the product state. The interaction energy is small but is responsible for a quite significant decrease of the activation free energy as compared to what is predicted by the simple theory of dissociative electron transfer. The source of the decrease of the activation barrier at the peak potential is illustrated in Figure 5, with the C- - -Cl distance-dependent potential energy curves for the reactant and products. The complete potential energy surfaces are more complicated, involving, in addition, the solvent reorganization coordinate. Since a minimum is present on the product potential energy surface, one may argue that, even if the minimum is shallow, electron transfer and bond breaking occur in two steps. In fact, the present situation is entirely different from a stepwise mechanism in which the intermediate ion radical on the reaction pathway is of much higher energy than the fragments.[1,2] In the present case, the bond is essentially broken at the product energy minimum, although the two fragments remain held together by a weak interaction of the charge−induced dipole type. The distinction between the stepwise and concerted mechanisms in the case of a small but distinct attraction between the fragments after bond breaking is illustrated by the potential energy profiles shown in Figure 6. The shallow energy minimum is present in the product state for both the concerted and the stepwise mechanisms. Concerning the passage from the former to the latter upon increasing the driving force offered to the reaction, the usual rules[2c,4,10b,18] apply in the present case, too.

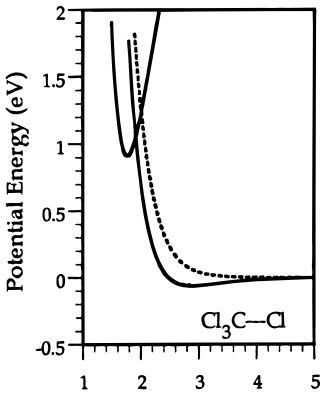

Figure 5. Reactant and products potential energy curves for the stretching of the C- - -Cl bond distance (in Å). For the product curves, the dotted line represents no interaction, and the full line represents −0.062 eV interaction.

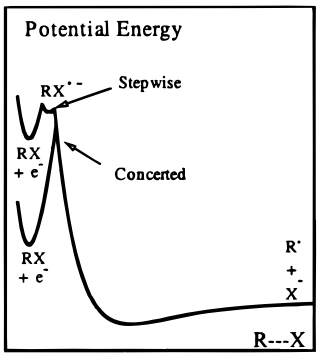

Figure 6. Potential energy profiles showing the distinction between the stepwise and concerted mechanism in the case of a small but distinct attraction between the fragments after bond breaking.

Conclusions

Our main conclusions are as follows. Analysis and modeling of the electrochemical reductive cleavage of CCl_4 in DMF reveals that it is, at least at low and moderate driving forces, a dissociative process in which electron transfer and bond breaking are concerted. A small but distinct attractive interaction, however, exists in the clustered fragments state, which facilitates the reaction in terms of both driving force and intrinsic barrier. It is remarkable that such a small interaction, of the order of 60 meV, is sufficient to produce a strong acceleration of the reaction.

(18) Severin, M. G.; Farnia, E.; Vianello, E.; Arévalo, M. C. *J. Electroanal. Chem.* **1988**, *251*, 369.

Methodology for Quantum Chemical Calculations

All calculations were carried out with the Gaussian 94 or Gaussian 98 packages.[19] The unrestricted Hartree−Fock method was used for all open-shell systems with a 6-31G* basis set. Correlation energy was introduced according to the Möller−Plesset perturbation treatment up to second order (MP2). All geometries were optimized at the MP2 level (calculations are quoted as either UHF-MP2 or MP2). No imaginary frequencies were found from the analytical second derivatives of the energies, confirming that stationary points are true minimum on the potential energy surface. The second derivatives were also used to obtain various thermodynamic parameters, including the zero-point energy and the entropy term from the usual relationships within the ideal gas, rigid rotor, and harmonic oscillator models. The standard enthalpies, free enthalpies, and molar entropies were corrected by a scaling factor (0.9646) applied to the zero-point energies and thermal energy corrections. The charges on the chlorine atom were obtained by a Mulliken population analysis.

Concerning carbon tetrachloride, the bond dissociation energy for the C−Cl bond was obtained as the ΔH^0 value of the reaction starting from CCl_4 and going to the two fragments $Cl^\bullet + CCl_3^\bullet$ (fully optimized at the MP2 level). An energy profile was calculated at the MP2 level for several values of the length of one C−Cl bond, around its equilibrium value. The other coordinates were then optimized under the constraint that the leaving chlorine atom remains in the axis of the pyramid formed by the three other chlorines. Care was taken that no contamination occurs from the triplet state at such interatomic distances. Indeed, its energy appears to be too high to interfere with the singlet at these distances.

Such an energy profile in the gas phase was also constructed for the $CCl_3^\bullet$,Cl^- cluster as a function of the C- - -Cl^- distance, by using the same methodology as that used previously. Energies were obtained from equilibrium C- - -Cl^- distance (2.44 Å) up to 4 Å. The energy corresponding to the fragments at infinite separation was obtained by adding the energies of Cl^- and $CCl_3^\bullet$. To ensure the validity of this approach, the energy minimum was calculated at various levels: PM3, UHF, MP3, and QCISD. The results obtained at the MP2 level are close to those obtained at higher levels, while the PM3 and UHF results describe very poorly the geometry of the minimum onto the surface. All along this gas-phase profile, free enthalpies of solvation were evaluated using the COSMO procedure (*co*nductor-like *s*creening *mo*del) as implemented in Gaussian 98, which is a continuum approach generating a polygonal surface around the system at the van der Waals distance. The energy at infinite separation of the two fragments was obtained by adding the free solvation enthalpies of $CCl_3^\bullet$ and Cl^-.

Experimental Section

Chemicals. *N*,*N*′-Dimethylformamide (Fluka, >99.5%, stored on molecular sieves and under an argon atmosphere), the supporting electrolyte NEt_4BF_4 (Fluka, puriss), carbon tetrachloride (Acros, 99.8%), and chloroform (Acros, 99.8%) were used as received.

Cyclic Voltammetry. The working electrode was a 3-mm-diameter glassy carbon electrode disk (Tokai) carefully polished and ultrasonically rinsed in absolute ethanol before use. In the high-scan-rate experiments we used a 10-μm-diameter carbon disk (Princeton Applied Research). The counter electrode was a platinum wire and the reference electrode an aqueous SCE electrode. The potentiostat, equipped with positive feedback compensation and current measurer, used at low or moderate scan rates, was the same as previously described.[20a] The instrument used with the ultramicroelectrode at high scan rates has been previously described.[20b] All experiments were done at 21 °C, the double-wall jacket cell being thermostated by circulation of water.

JA001258S

(19) (a) Frisch, M. J.; Trucks, G. W.; Schlegel, H. B.; Gill, P. M. W.; Johnson, B. G.; Robb, M. A.; Cheeseman, J. R.; Keith, T.; Petersson, G. A.; Montgomery, J. A.; Raghavachari, K.; Al-Laham, M. A.; Zakrzewski, V. G.; Ortiz, J. V.; Foresman, J. B.; Cioslowski, J.; Stefanov, B. B.; Nanayakkara, A.; Challacombe, M.; Peng, C. Y.; Ayala, P. Y.; Chen, W.; Wong, M. W.; Andres, J. L.; Replogle, A. S.; Gomperts, R.; Martin, R. L.; Fox, D. J.; Binkley, J. S.; Defrees, D. J.; Baker, J.; Stewart, J. P.; Head-Gordon, M.; Gonzalez, C.; Pople, J. A. *Gaussian 94*, Revision E.1; Gaussian, Inc.: Pittsburgh, PA, 1995. (b) Frisch, M. J.; Trucks, G. W.; Schlegel, H. B.; Scuseria, M. A.; Gill, P. M. W.; Johnson, B. G.; Robb, M. A.; Cheeseman, J. R.; Keith, T.; Petersson, G. A.; Montgomery, Stratmann, R. E.; Burant, J. C.; Dapprich, S.; Millam, J. M.; Daniels, A. D.; Kudin, K. N.; Strain, M. C.; Farkas, O.; Tomasi, J.; Barone, V.; Cossi, M.; Cammi, R.; Mennuci, B.; Pomelli, C.; Adamo, C.; Clifford, S.; Ochterski, G.; Cui, Q.; Morokuma, K.; Malick, D. K.; Rabuck, A. D.; J. A.; Raghavachari, K.; Al-Laham, M. A.; Zakrzewski, V. G.; Ortiz, J. V.; Foresman, J. B.; Cioslowski, J.; Stefanov, B. B.; Liu, G.; Liashenko, A.; Piskorz, P.; Komaromi, I.; Nanayakkara, A.; Challacombe, M.; Peng, C. Y.; Ayala, P. Y.; Chen, W.; Wong, M. W.; Andres, J. L.; Replogle, A. S.; Gomperts, R.; Martin, R. L.; Fox, D. J.; Binkley, J. S.; Defrees, D. J.; Baker, J.; Stewart, J. P.; Head-Gordon, M.; Gonzalez, C.; Pople, J. A. *Gaussian 98*, Revision A.1; Gaussian, Inc.: Pittsburgh, PA, 1998.

(20) (a) Garreau, D.; Savéant, J.-M. *J. Electroanal. Chem.* **1972**, *35*, 309. (b) Garreau, D.; Hapiot, P.; Savéant, J.-M. *J. Electroanal. Chem.* **1989**, *272*, 1.